Summary of the geological evolution of Syria through geophysical interpretation: Implications for hydrocarbon exploration

GRAHAM E. BREW, ROBERT K. LITAK, DOGAN SEBER, MUAWIA BARAZANGI, Cornell University, Ithaca, New York
TARIF SAWAF, ANWAR AL-IMAM, Syrian Petroleum Company, Damascus, Syria

Intracontinental deformation, caused by plate boundary processes, dominates the past and present tectonics of Syria (Figure 1). This deformation has created structures that form hydrocarbon traps in several different areas of the country. Current production from Syria is around 600 000 b/d and the country hosts ongoing exploratory efforts. Deformation within Syria can be conveniently divided into four zones (Figure 2): the Dead Sea fault system; the Palmyride fold and thrust belt; the Euphrates fault system; and the Abd el Aziz/Sinjar structures in the northeast. Each has been, and continue to be, studied in detail by the Cornell Syria Project, an industry-sponsored collaborative program between Cornell and Syrian Petroleum Company (SPC) scientists that uses diverse geophysical and geological data to analyze the tectonics of the northern Arabian platform.

Early work focused mainly on the Palmyrides. Research included seismic reflection interpretation, construction of balanced cross-sections, gravity modeling and more. The Palmyrides are a Mesozoic rift, inverted in the Late Mesozoic and Cenozoic. It was concluded that deformation within the Palmyrides varies considerably along strike, from predominately thin-skinned deformation with relatively high amounts of shortening (about 10-20 km) in the southwest, to thick-skinned deformation with almost no shortening in the northeast (Figure 3). The present-day Palmyrides are host to a number of gas-producing fields with trapping within inversion structures.

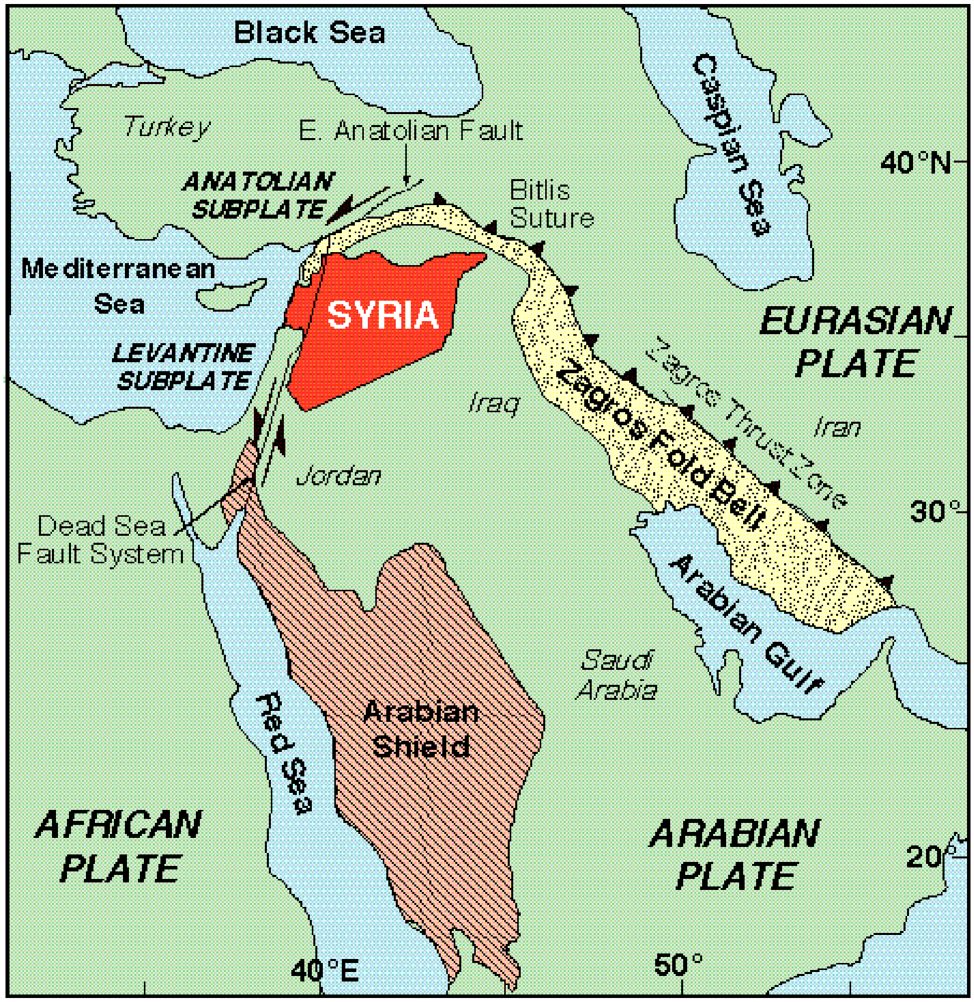

Figure 1. Regional tectonic setting of Syria. Intraplate deformation in Syria is controlled by movements on the Arabian plate boundaries that surround much of the country.

Editor's note: A version of this paper won the Best Student Poster at the 1996 SEG Annual Meeting in Denver.

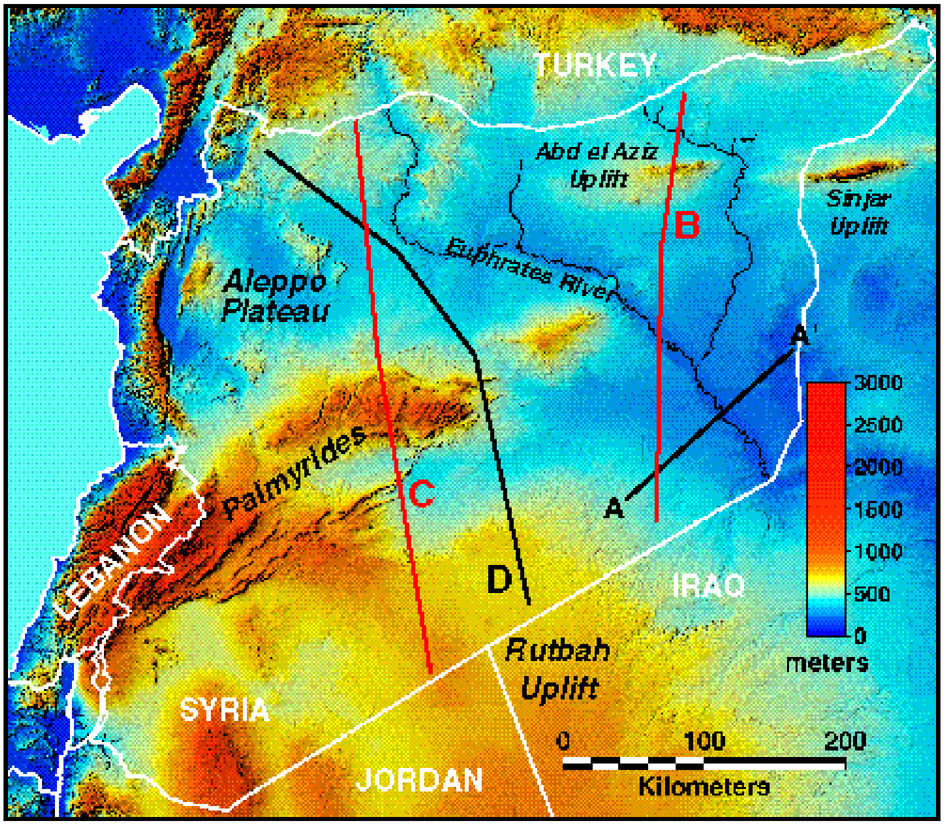

Figure 2. Topography of Syria and surrounding regions. This high resolution topographic image shows the main structural zones of Syria. Note the Dead Sea fault system in the west, the Palmyrides, the Euphrates river that reflects the underlying Euphrates fault system, and the deformation in the northeast of the country. Line A-A' is the location of the cross section in Figure 6. The refraction profile interpreted in this article is along line B. Profile C is a similar refraction profile that was interpreted previously with the results in Figure 15. The location of the gravity modeling shown in Figure 17 is along line D.

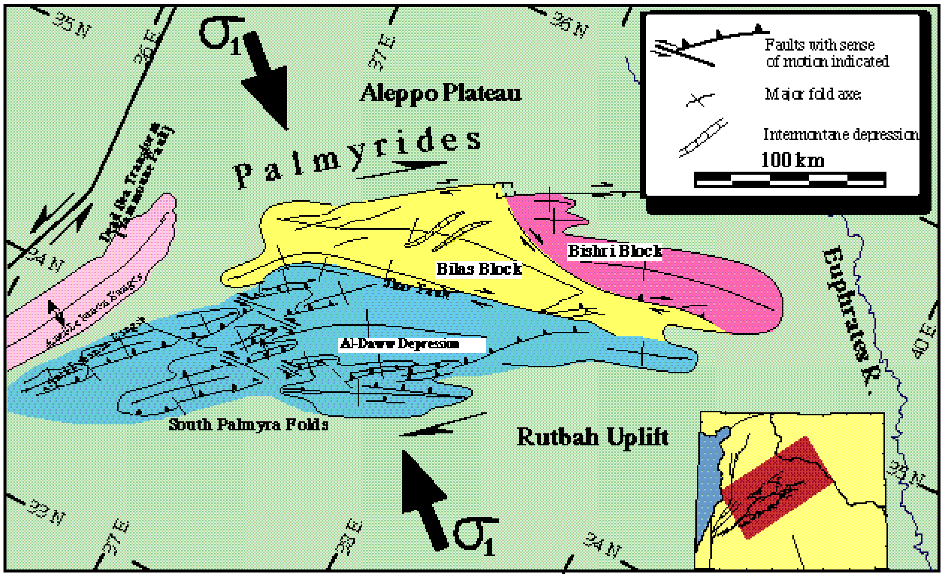

Figure 3. Simplified kinematics of the Palmyrides. Major faults with established sense of displacement are shown. Compression is most likely predominant in the deformation of the area, although the proportion of strike-slip vs. compressional tectonics is as yet unknown. Arrows show likely direction of maximum compressive stress based on orientation of structures and earthquake focal mechanisms.

The left-lateral Dead Sea fault system extends from the Gulf of Aqaba to the Cyprus subduction zone/Bitlis suture/Dead Sea transform triple junction in the north. Research shows that the northern segment of the fault, north of the Anti-Lebanon Ranges (Figure 3), has seen much less offset than the fault in the south. Current studies are using satellite imagery (Figure 4), high resolution topography (Figure 2) and seismic reflection data to establish the timing and style of deformation along the northern segment of the fault. These findings will be used to establish why the northern and southern segments of the fault have seen such different histories. On a more regional scale, Landsat Thematic Mapper imagery of the entire northern Arabian platform is currently being processed and analyzed at Cornell, and forms an integral part of our research efforts.

The Euphrates has been the subject of intensive study by the project in recent years. This is particularly relevant given the initiation of appreciable petroleum production from the Euphrates dating from the early 1980s (Figure 5). Again using

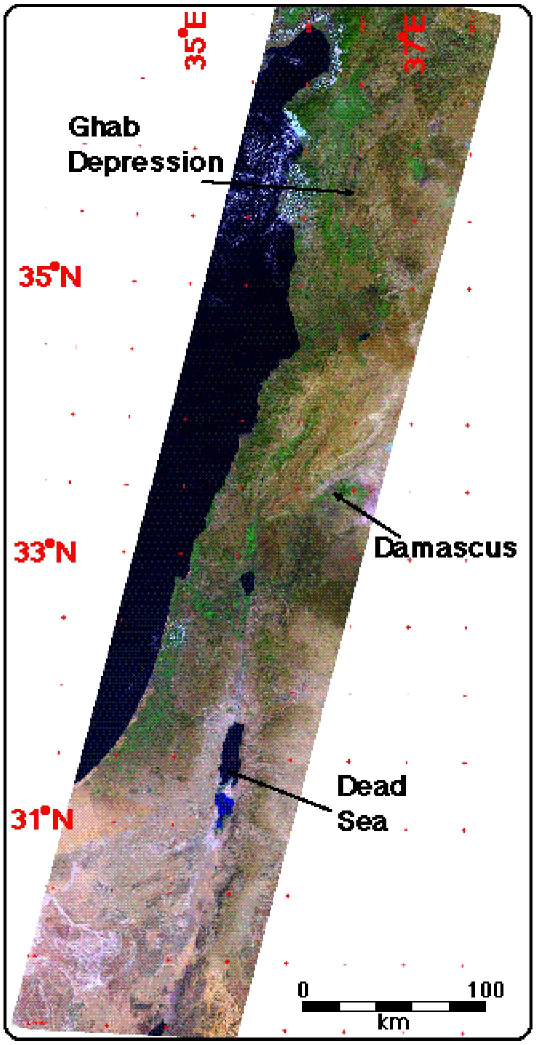

Figure 4. Landsat Thematic Mapper image of Dead Sea fault system. Spectral bands in this false color image are 1 (visible blue, displayed in the figure as red), 4 (near infrared; green), and 7 (mid infra-red; blue). The branching of the fault system, and the numerous pull-apart basins, as well asother features of the fault zone, are visible in this image.

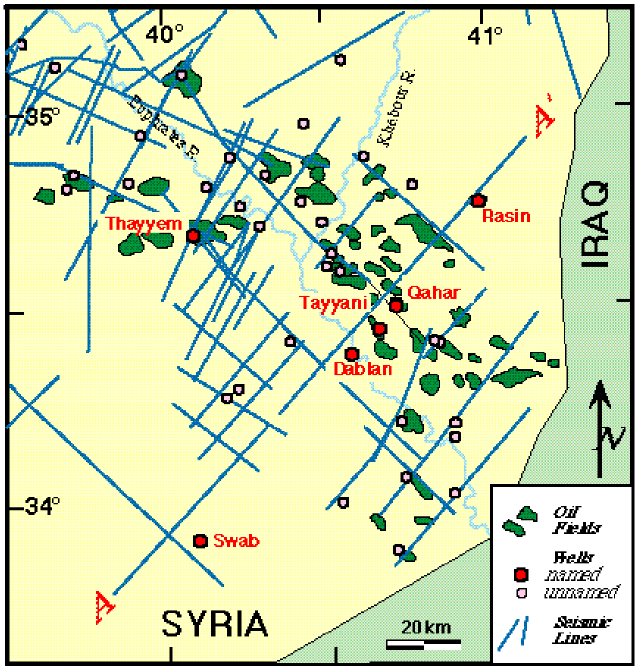

Figure 5. Database used in Euphrates research. Shown here are the locations of principal oil fields, wells and seismic reflection data in the Euphrates area. Estimates of recoverable oil reserves discovered in the Euphrates graben are currently over 1 billion barrels.

a variety of geophysical and geological data, mapping of horizons and analysis of structures was performed along the length of the Euphrates from the Iraqi border to Turkey in the north. This yielded a picture of complex and changing deformation along the Euphrates (Figure 6). Deformation is distributed and has changed from transpressional to transtensional over time. Figure 7 shows that previously-supposed simple rift bounding faults are not present. Using results from the Euphrates and Palmyrides research, a preliminary picture of Syrian tectonics since the Triassic has been constructed (Figure 8).

Current and future studies will use seismic reflection data to analyze the tectonics of northeast Syria, in particular the Abd el Aziz and Sinjar structures (Figure 2). Deformation here appears to be contemporaneous with movements in the Euphrates and the Palmyrides, and can probably be attributed to the same plate boundary events. Cretaceous rifting and Plio-Pleistocene inversion have created hydrocarbon traps in Mesozoic and Cenozoic strata. Through construction of structure maps, isopachs and cross-sections, the evolution of the area will be studied back into the Paleozoic.

Whilst most previous hydrocarbon discoveries in Syria have been in Mesozoic and Cenozoic rocks, current exploration is overwhelmingly focused on the Paleozoic. Silurian shale source rocks have been documented in many parts of the country, and Ordovician and Carboniferous sandstones could form useable reservoirs. Knowledge of the Paleozoic in Syria is sparse, however, owing to appreciable thicknesses of younger sedimentary cover. Very few Paleozoic outcrops exist and, based on current knowledge, no well in Syria has penetrated the entire sedimentary section down to metamorphic basement.

The study detailed here uses refraction data and other data sources to determine basement depth and deep sedimentary structure in eastern Syria, yielding results relevant to both issues of Paleozoic prospecting and the regional tectonics of Syria.

Basement depth in eastern Syria. The primary data of this study were a refraction profile collected during 1972-3 (Figure 9). The geometry of the survey led to highly detailed results compared to the standard for refraction surveying today. Records from 23 reversed shots were studied along the profile's 302 km, yielding an overlap of at least seven recordings in most parts of the line (Figure 10). Geophone spacing was 150 ms, and shot sizes of up to and above one ton lead to clear first arrivals even out to the ends of the spreads. The nominal spread length was 48 km and the maximum 54 km. First arrival times were digitized.

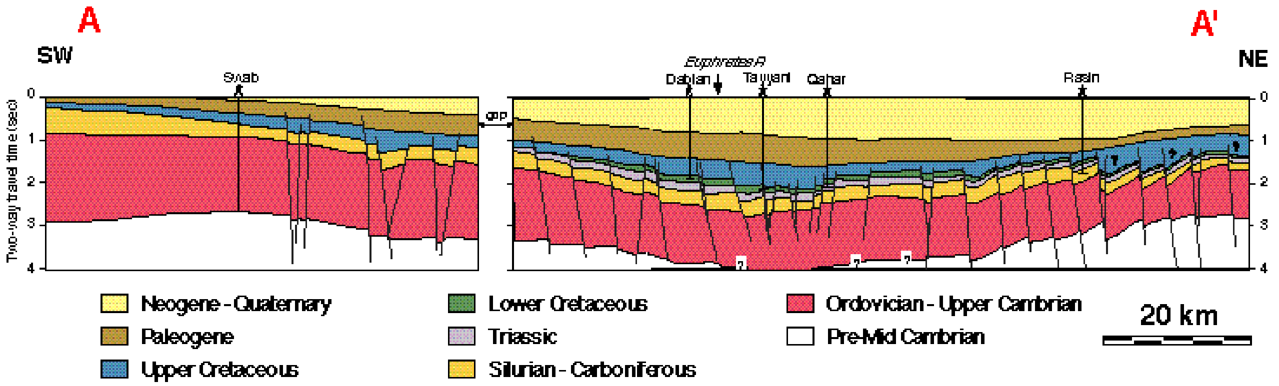

Figure 6. Cross-section across the Euphrates graben. Location of cross-section is shown on Figures 2 and 5. This cross-section is constrained by seismic and well data. Note the numerous faults, with only the larger ones shown here, demonstrating the distributed nature of deformation in the graben. Dramatic thickening of the Upper Cretaceous strata indicates that the rifting was most active at this time, followed by a period of Paleogene post-rift subsidence.

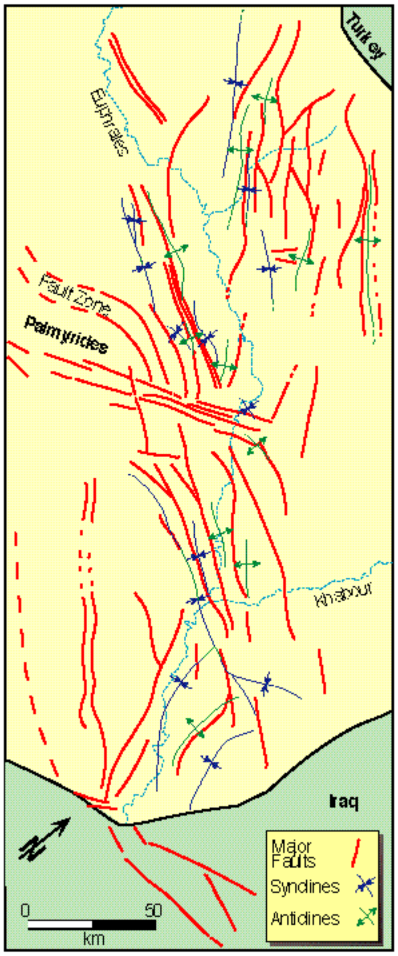

Figure 7. Structural framework of the Euphrates fault system. The Euphrates fault system extends from the Iraqi boarder in the southeast and approaches the Turkish border in the northwest. Many faults have experienced a variety of normal, thrusting and strike-slip movements; hence offsets are not shown.

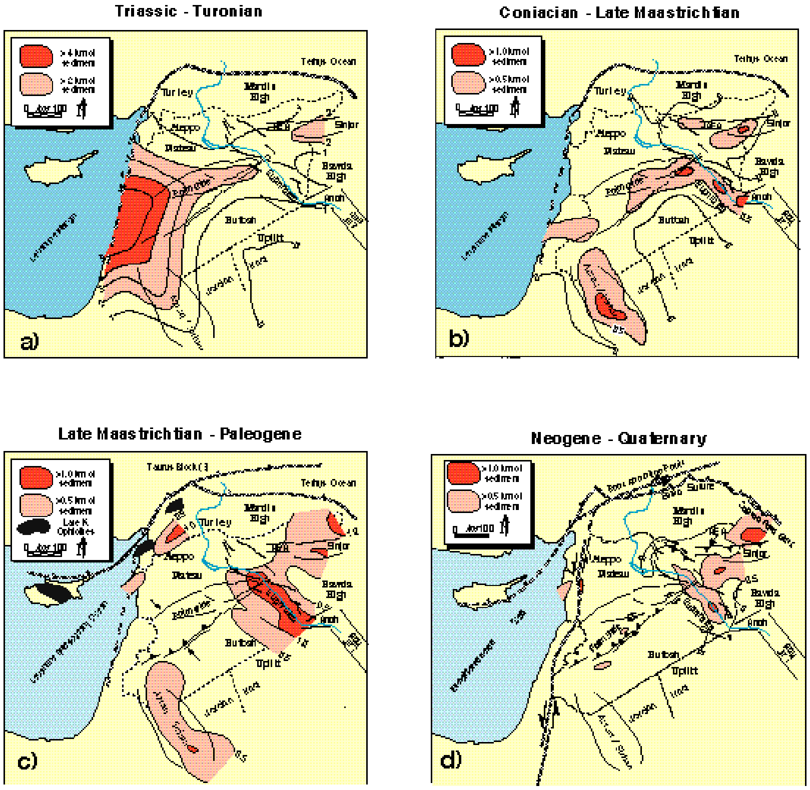

Figure 8. Evolution of the northern Arabian platform. Generalized isopachs and proposed tectonic setting of Syria and surroundings from Triassic to Recent. Present-day geography retained. AEA = Abd el Aziz. (a) Major deposition along the Levantine margin and within the Palmyride/Sinjar trough. (b) Decreased deposition on the Levantine margin, increased deposition in the Sinjar, southern Euphrates and Sirhan areas. (c) Collision along the northwest margin of Arabia leads to inversion of the Palmyrides and termination of rifting in the Euphrates. (d) Full-scale collision along the northern margin leads to transpression in the Palmyrides and Euphrates, and compression in the Sinjar and Anah areas.

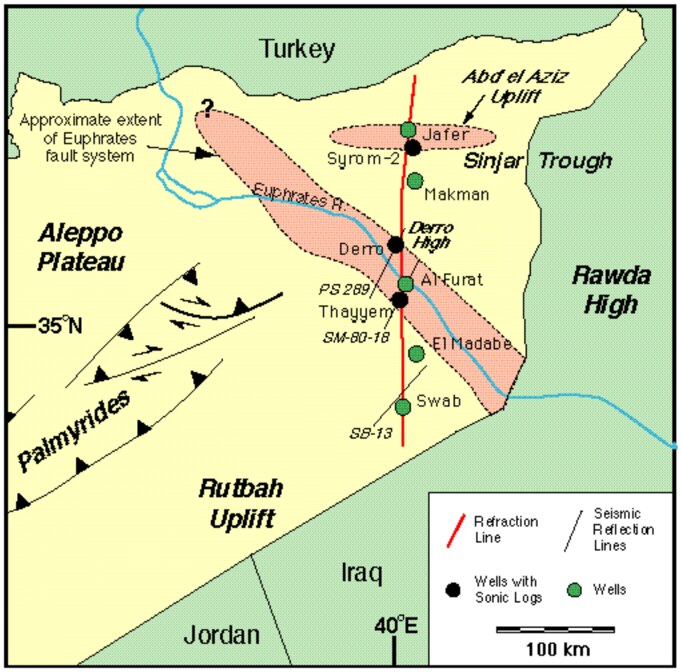

Figure 9. Location of data in eastern Syria. The seismic refraction profile extended more than 300 km through eastern Syria across the Euphrates fault zone. Also indicated are other coincident data (seismic reflection data and well data) used to constrain the velocity interpretation.

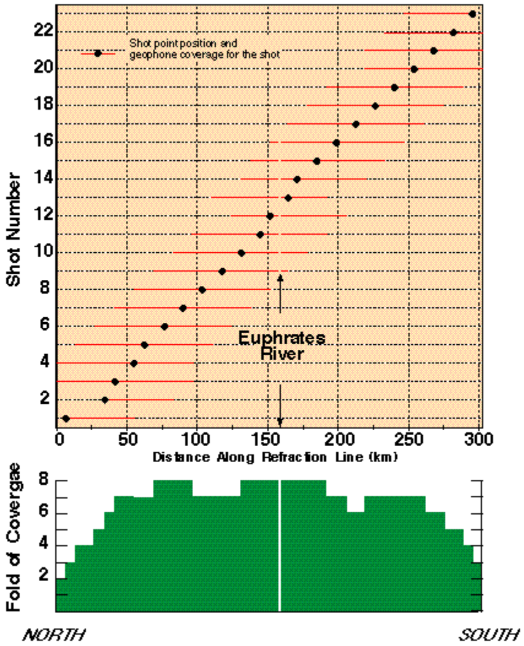

Figure 10. Geometry of the refraction survey. The highly detailed nature of the refraction acquisition led to an overlapping fold of coverage of at least 700% in most places. Nominal spread length of the survey was 48 km, with the greatest offset being 54 km. First arrival times from 23 shots were used in the interpretation.

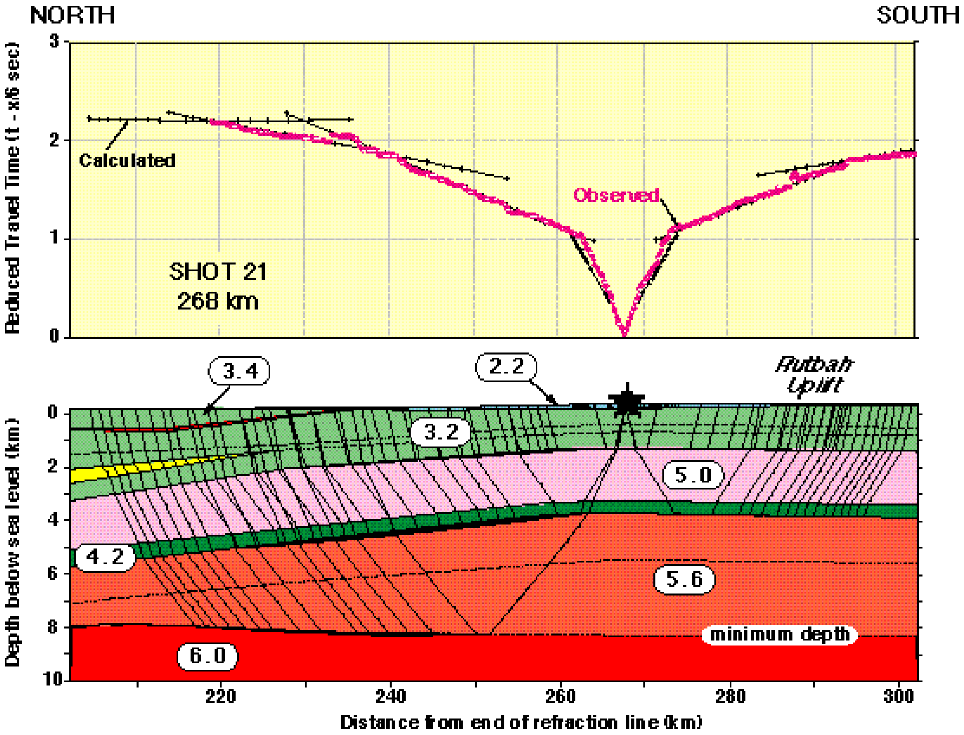

Figure 11. Ray-tracing interpretation. Example of ray-tracing a shot and showing the fit between the modeled and the observed arrival times. The velocity model used in this example is the final velocity model as shown in Figure 14. Thus the fit here between observed and calculated arrivals is the optimum we obtained for this shot, and is fairly representative of the fits for all other shots.

To derive a complete velocity model beneath the refraction profile a ray-tracing approach was used. The refraction data could have been used singularly in this effort, but we had access to much more data coincident with the refraction profile, including reflection profiles and well data (Figure 9), and so these were integrated into the modeling effort.

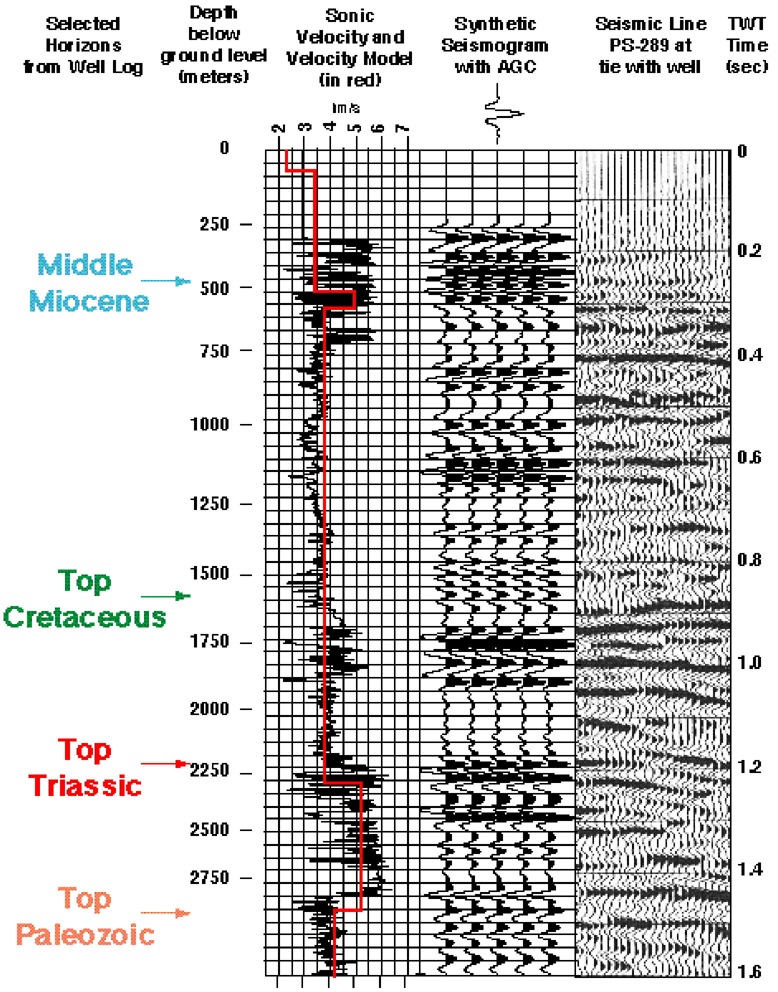

Figure 12. Well data. Sonic log, synthetic seismogram and actual seismic reflection data at the Derro well are shown superposed with velocities from the refraction data (thick red line). Well data were used to constrain the refraction data in areas of low velocity zones, for example beneath the high velocity mid-Miocene evaporites.

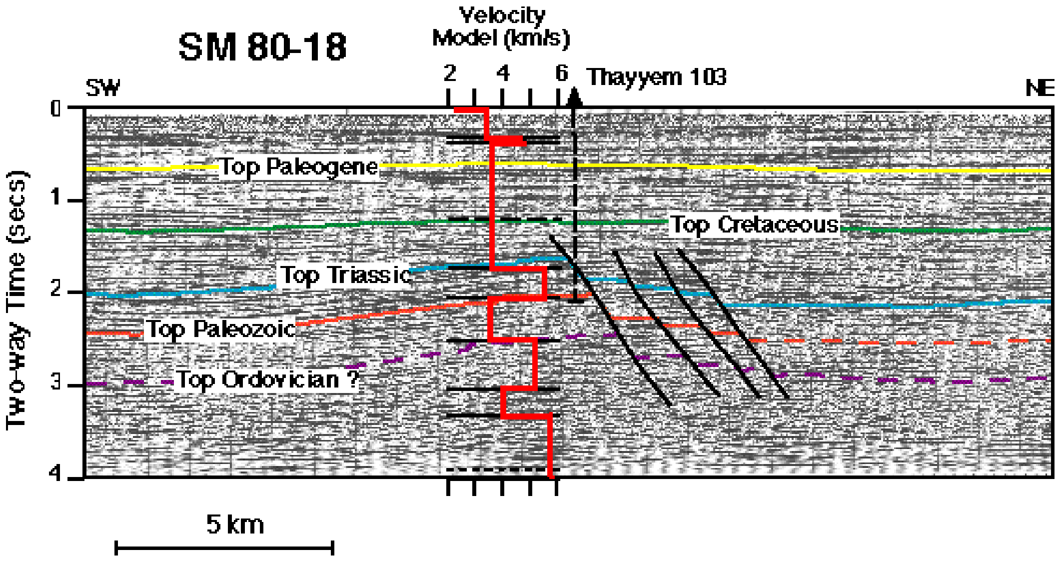

Figure 13. Seismic reflection line coincident with refraction profile. In this figure the final velocity model (red line) is superposed on reflection data from the same point on the southern edge of the Euphrates graben (see Figure 9 for location). Several velocity interfaces identified by refraction data are prominent reflectors. Seismic reflection data were used to improve the resolution of the velocity model in certain areas. The Thayyem well shown is one of the most prolific oil-producers in the Euphrates.

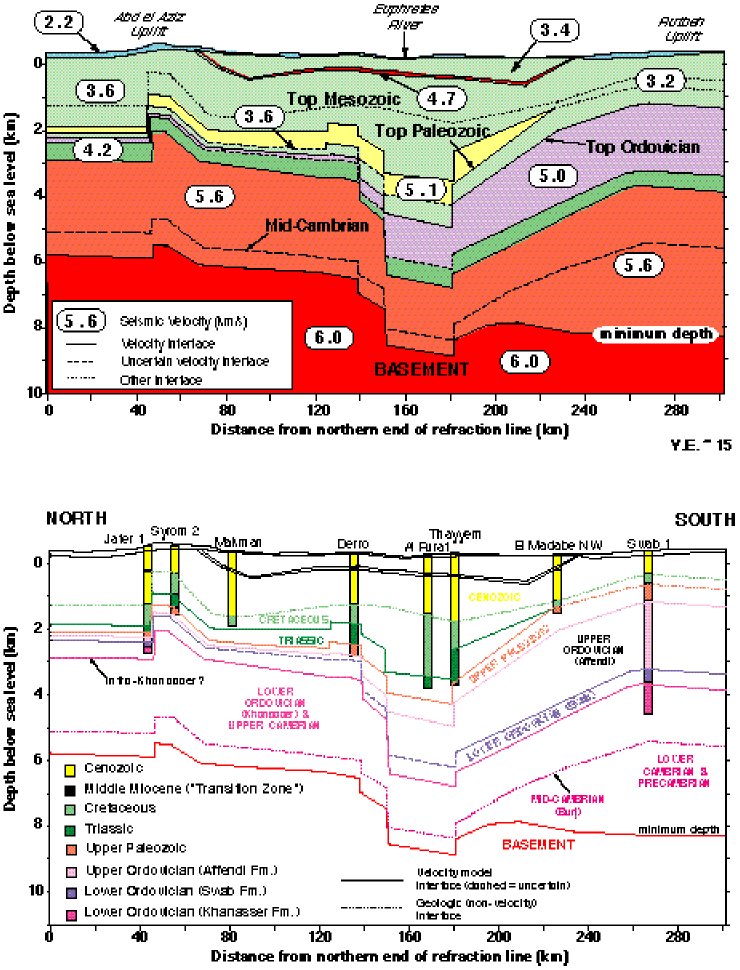

Figure 14. Final velocity model derived from data analysis. This figure shows the velocity structure of the sediments beneath the refraction profile. The velocities have been derived from an integrated interpretation of the refraction data with constraints and enhancements from other coincident data sources. Seismic velocities of 6 km/s are taken to represent basement rocks. Due to the limitations of the survey geometry, basement depth as shown in the south only has a minimum constraint. In the lower figure the velocity interfaces are shown superposed on the well data from along the profile (see Figure 9 for location). In general we see a close agreement between the location of the velocity interfaces and prominent stratigraphic boundaries.

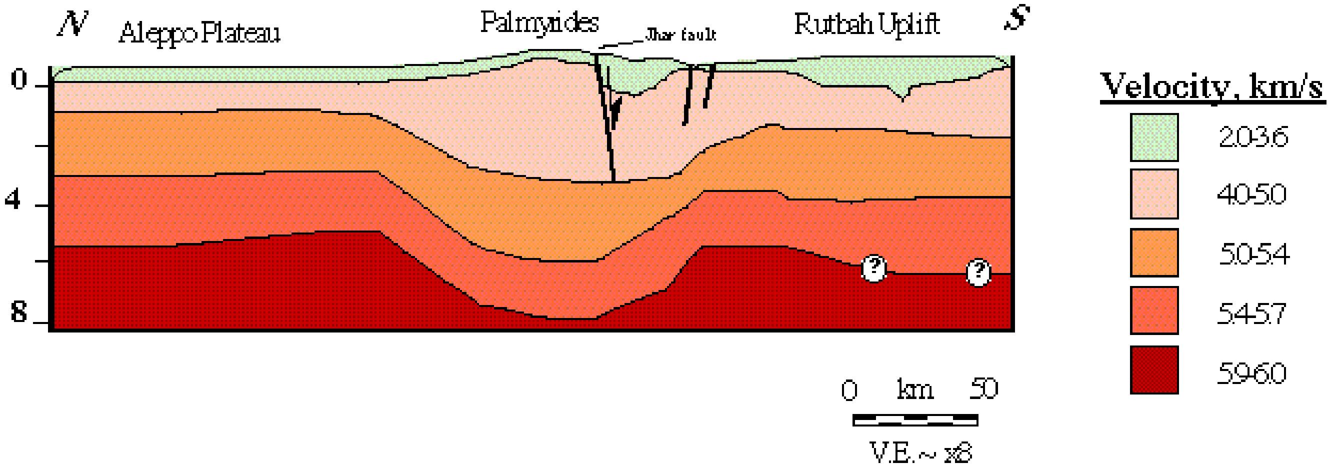

Figure 15. Previous refraction results. These are the results of a previous refraction interpretation in central Syria (see Figure 2 for location). We see that the deepest basement is beneath the Palmyrides, where a large trough remains predominately uninverted. Additionally, we see deeper basement on the southern end of the profile relative to north of the Palmyrides. Similar to the refraction work in the east of Syria, basement depths on the southern end of the profile are minimum constraints because the survey geometry was insufficient to sample first arrivals from the basement.

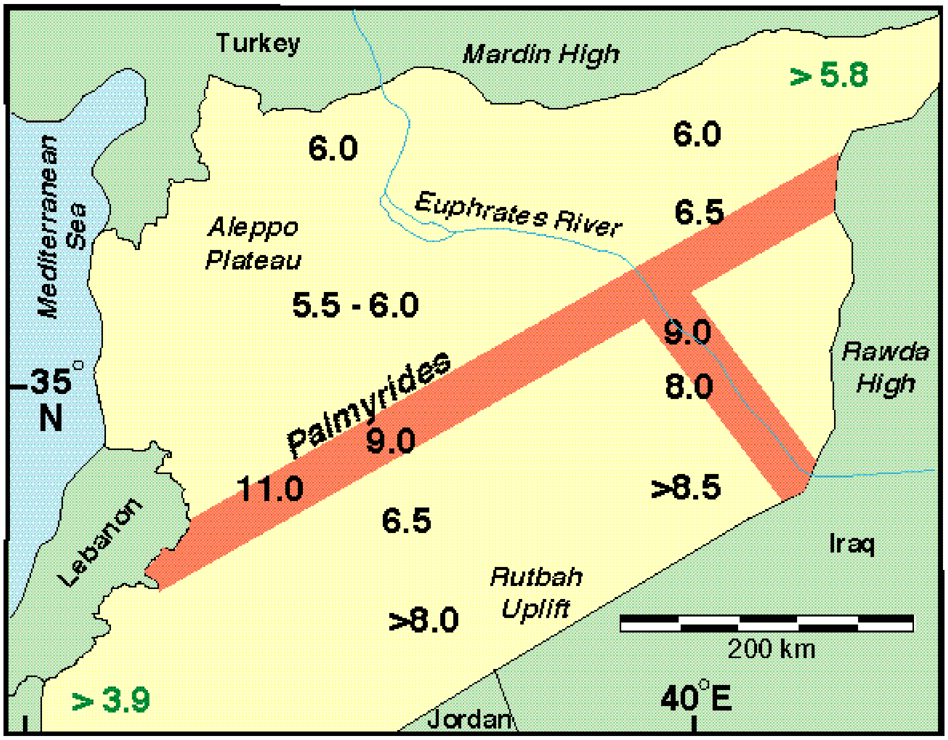

Figure 16: Basement depth in Syria. This summarizes current knowledge of basement depth in Syria in kilometers below surface. Black data points are from refraction data, green are minimum constraints from selected well data. No wells in Syria have penetrated basement rocks. Colored zones are the hypothesized locations of shear/suture zones, likely from the Pre-Cambrian, that could still be controlling the regional deformation within Syria.

An example of the ray-tracing modeling is shown in Figure 11. The velocity model shown in this figure is the final velocity model and the fit between the observed and calculated arrivals shown in Figure 11 is typical for the fit along the entire profile. The velocity model was altered to improved this fit one shot at-a-time. At the same instant, the velocity model was compared to well data (Figure 12) and seismic reflection data (Figure 13) in order to constrain and improve the model.

This interactive, integrated modeling procedure led to a velocity model that fitted all the available data (Figure 14). Note that basement depth in the south of the profile is a minimum estimate, as even the farthest geophone offsets used here were not long enough to sample refractions from the basement as first arrivals. The main conclusions that can be drawn from these results in Figure 14 are:

1) Depth to metamorphic basement in eastern Syria is much greater than previously estimated.
2) The Paleozoic sedimentary section, the current focus for oil exploration in eastern Syria, is between 3 km in the north to over 4.5 km thick in the far south.
3) There are dramatic differences in basement depth on either side of the Euphrates graben system.
4) Deformation in the Euphrates fault system is basement involved and shows no dramatic signs of inversion.
5) Although seismic velocity generally increases with depth, velocity is also controlled by lithology and low velocity zones occur within the section.
6) Most of the identified velocity contrasts can be associated with significant age boundaries (Figure 14).

We can incorporate the results of this study with findings from previous refraction work (Figure 15) and well data to derive a map of basement depth throughout Syria (Figure 16). This shows that the deepest basement occurs in the deformed zones of the Euphrates and the Palmyrides. Also, basement depth south of these features beneath the Rutbah uplift is consistently deeper than the basement in the north of Syria.

It is suggested here that this difference in basement depth could be a consequence of fundamentally different geologic history on either side of the Palmyrides and Euphrates. The Palmyride and Euphrates trends could represent suture or shear zones along which the northern Arabian platform accreted during Late Proterozoic time. These suture/shear zones could be acting as zones of weakness that still influence the intracontinental deformation of Syria.

The suturing hypothesis is supported by gravity modeling. Gravity modeling along a transect across the Palmyrides concluded that the difference in gravity signature on either side of the mountains could be explained by differences in lower crustal densities or thicknesses (Figure 17). Comparable modeling across the Euphrates yielded similar results. Although nonunique, the basement depth and gravity observations, when considered in totality, support the hypothesis of weak zones dating back to the Proterozoic beneath the sedimentary cover in Syria that still affect regional tectonics. These hypothetical zones are shown on Figure 16.

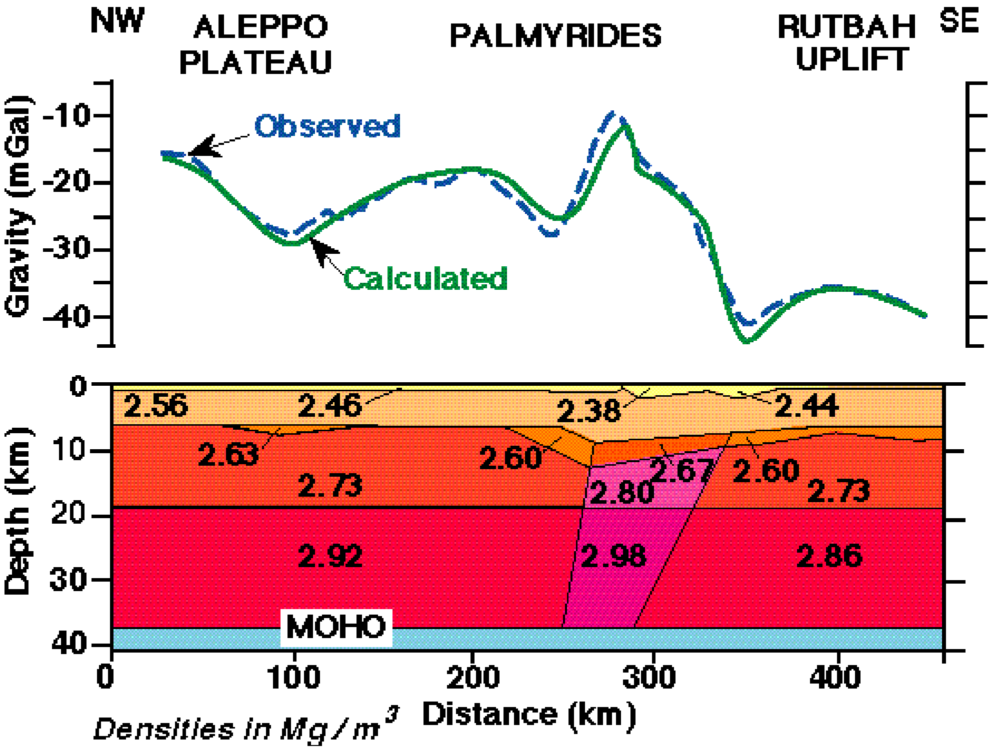

Figure 17. Gravity modeling across the Palmyrides. This figure demonstrates that the gravity signature across the Palmyrides (see Figure 2 for location) can be explained by differences in the density and/or thickness of the lower crust. Similar results were obtained from gravity modeling across the Euphrates. Such findings support the hypothesis that the northern Arabian platform accreted from several distinct continental blocks. The suture/shear zones between these blocks could still be acting as weak zones along which intraplate deformation is occurring.

Summary. The work presented here is a typical sample of the research conducted by the Cornell Syria Project, which can be seen as a model of joint cooperative work between a national oil company (Syrian Petroleum Company) and an academic research group (Cornell University), with sponsorship from the oil industry. Using diverse geophysical and geological data sets, the Project aims to address issues concerning the tectonic evolution of the northern Arabian platform, with results that are directly relevant to hydrocarbon exploration in Syria and surrounding areas. For more information about the Syria project, see our Web page at http://atlas.geo.cornell.edu/syria/welcome.html

Suggestions for further reading. “Tectonic evolution of the northern Arabian plate in western Syria” by Barazangi et a. (in Recent evolution and Seismicity of the Mediterranean Region, Kluwer, 1993). “Bouguer gravity trends and crustal structure of the Palmyride Mountain belt and surrounding northern Arabian platform in Syria” by Best et al. (Geology, 1990). The Middle East: Regional Geology and Petroleum Resources by Beydoun (Scientific Press Limited, 1988). “Basement depth and sedimentary velocity structure in the northern Arabian Platform, Eastern Syria” by Brew et al. (Geophysical Journal International, 1997). “Mesozoic-Cenozoic evolution of the Euphrates fault system, Syria: Implications for regional kinematics” by Litak et al. (Jounal of the Geological Society of London, 1997). “Upper crustal velocity structure and basement morphology beneath the intracontinental Palmyride fold-thrust belt and north Arabian platform in Syria” by Seber et al. (Geophysical Journal International, 1993).

Acknowledgments: This work was supported by Amoco, ARCO, Conoco, Exxon and Mobil. We thank Weldon Beauchamp and Francisco Gomez, both at Cornell, for valuable advice and assistance.

Corresponding author: Graham Brew, 607-255-5514, brew@geology.cornell.edu